Current Topics in Colloid & Interface Science
Vol. 7, 2006

Original Communication

Preparation and characterization of conducting polymer shell / core composite nanoparticles

Frederic Prulliere, Gyu Leem, Nathaniel C. Reisinger and T. Randall Lee*

Department of Chemistry, University of Houston, 4800 Calhoun Road, Houston, Texas 77204-5003, USA

ABSTRACT

Dielectric particles coated with conducting polymer shells were synthesized because of their potentially useful optical properties, such as optical absorbances in the UV-vis to mid-infrared region and enhanced third-order nonlinear optical properties. Polyaniline and polypyrrole coatings were grown by dispersion polymerization *in situ* with silica and polystyrene core particles that ranged from 200 nm to 2 μm in diameter. Discrete polypyrrole shells were grown on sub-micrometer silica cores as well as polypyrrole and polyaniline shells on micrometer silica and polystyrene cores. The addition of a steric stabilizer to the core particles was needed to form discrete shells. The conducting polymer shell/core composite particles were characterized by scanning electron microscopy, FT-IR spectroscopy, and UV-vis spectroscopy.

KEYWORDS: conducting polymer, dielectric, shell/core, composite nanoparticles

INTRODUCTION

With the increasing need to manipulate optical signals in fiber-optic communications and in parallel optical image-processing systems, optical devices with enhanced performance capacities are required. Indeed, the current chemical composites used in integrated optical devices and in the frequency conversion of lasers (e.g., inorganic compounds such as lithium niobate, potassium dideuterium phosphate, and potassium titanyl phosphate) [1, 2] are fragile and undergo degradation upon exposure to light. Thin layers of conducting polymers offer an inexpensive and robust alternative with surface-plasmon resonance and semiconducting capacities, in addition to strong nonlinear optical properties (e.g., high values of χ^3).

In conducting polymers, most, if not all, of the useful optical properties arise from the extended π conjugation along the polymer backbone. Thus, β-carotene and retinal were among the first systems studied [3]. These specific organic structures, however, cannot be readily used in device fabrication due to their poor crystallinity, toilsome processability, and extreme fragility. We believe that certain derivatives of conducting polymers having shell/core geometries that can be used as alternative materials. In particular, the emergence of conducting polymer shell/core nanostructures should provide easy access to optically-active transparent thin films [4-8].

In the work reported here, we explored the growth of a conducting polymer shell around a dielectric core nanoparticle. The resultant composite particles are expected to exhibit a tunable plasmon resonance in the near infrared region of the spectrum [9]. We are precisely targeting wavelengths in the 700-1100 nm range for biological applications, given that the human body possesses few or no chromophores that are strongly active within this region of the spectrum [10]. Tunable plasmon resonances have been previously observed in related Au shell/dielectric core and Ag shell/ dielectric core nanoparticle architectures [11-16]. In these systems, the plasmon band can be shifted from ~600 nm to more than 1000 nm simply by

*Corresponding author.
trlee@uh.edu

changing the shell-thickness to core-size ratio. We wished to extend this concept to conducting polymer layers on dielectric cores because the plasmon resonance of most doped conducting polymers falls within the near infrared region, which should allow ready access to even longer absorption wavelengths, and thus use in applications requiring infrared filters or blocking agents. Various conducting polymer nano-structures having shell/core geometries have been reported [17-20]. With one exception [21], the various synthetic methods typically afford a mixture of coated and uncoated cores, as well as inhomogeneously coated cores.

Because of their stability and optical properties [9], we chose polyaniline and polypyrrole for use as conducting-polymer overlayers. Armes and co-workers developed a method for synthesizing polymeric shell/core composite particles in the micrometer size range [21]. In their method, sterically-stabilized latex particles were successfully coated with a thin layer of conducting polymer. In the work reported here, we explore the Armes route and other routes for preparing discrete polyaniline and polypyrrole shells on submicron- and micron-sized silica and polystyrene cores using a variety of methods for polymer growth and particle stabilization. We characterize the resultant structures and their optical properties through the use of scanning electron microscopy (SEM), FT-IR, and UV-vis spectroscopy.

EXPERIMENTAL SECTION

Materials

All reagents were purchased from the indicated suppliers and used without further purification unless noted otherwise: sodium hydroxide, ammonium hydroxide, hydrochloric acid, hydrogen peroxide, and potassium persulfate (all from EM Sciences); styrene, aniline, and pyrrole (all from Acros); iron chloride, potassium iodate, copper nitrate, polyethylene glycol 30000, polyvinyl alcohol, and methoxy-capped polyethylene glycol methacrylate (all graciously donated by Laporte Chemicals); tetraethylorthosilicate (Aldrich); polyvinylpyrrolidone PVK 30 (Fluka); and Polybead® 2.5 μm latex beads (Polysciences). The solvents, absolute ethanol (McKormick Distilling) and isopropanol (EM Sciences), were purchased from the indicated suppliers and used without further purification. Deionized water was carefully purified by passage through Millipore® organic and ionic cartridges.

Characterization methods

We used a JEOL JSM6400 scanning electron microscope operating at 15 keV to collect the SEM images. The preparation of the samples for analysis was straight forward: solutions containing the nanoparticles samples were added dropwise onto adhesive double-faced carbon tape, which was attached to a carbon pellet. The sample was allowed to dry overnight at room temperature to remove all traces of water before analysis.

All FT-IR data between 400 and 4000 cm^{-1} were collected using a Nicolet MAGNA-IR 860 spectrometer. For each sample, data were collected from 16 scans at a resolution of 1 cm^{-1}. The powdered samples were dispersed into anhydrous potassium bromide (typically 1 mg of sample in 100 mg of potassium bromide) and pressed into a pellet for analysis.

Over the range of 400 to 1100 nm, UV-vis spectra were collected using a Varian CARY 50 Scan UV-vis spectrometer. Samples were dispersed in either ethanol or water and loaded into a quartz cell. The background signal of the solvent was eliminated by subtraction. Over the range 175 to 3000 nm, UV-vis spectra were collected on finely divided powdered samples by attenuated total reflectance (ATR) using a Varian CARY 500 Scan UV-vis spectrometer. For each sample, data were collected for 32 scans at a resolution of 1 cm^{-1}.

Preparation of bare silica core nanoparticles

The silica cores were prepared using the traditional Stöber method [22]. Typically, 50 mL of absolute ethanol was poured into a 100-mL round-bottomed flask. Under strong agitation with a magnetic stirring bar (confirmed by the presence of a vortex), 3 mL of ammonium hydroxide (NH_4OH, 30% v/v in H_2O) was added to the flask. The mixture was stirred for 5 min, and 1.5 mL of tetraethylorthosilicate (TEOS) was added immediately. The flask was covered with a septum to avoid any change of concentration by evaporation. After an induction time of 10 to 30 min, the solution changed from colorless to opalescent

white, indicating the nucleation of the particles. The reaction was allowed to proceed overnight, and the silica nanoparticles were isolated in pure form using the following procedure. The mixture was poured into a 50-mL plastic centrifuge tube, and the particles were washed with Milli-Q water and ethanol during repeated centrifugations and redispersions. The centrifugations were performed at 2500 rpm using a Sorvall Instruments RC-3B refrigerated centrifuge. The particles were redispersed using a Branson 5210 sonication bath. The particles obtained using this method were spherical with 125 ± 15 nm diameters. To prepare particles with larger diameters, the TEOS/NH_4OH/ethanol ratio was varied as described [23]. The particles can be stored for an extended period of time without visible aggregation.

Preparation of SAM-coated silica cores and subsequent polyaniline shell growth

To functionalize fully the surface of the silica particles with an aniline-terminated SAM from which to grow polyaniline, we needed to estimate the total surface area and the number of reactive sites per area of a chosen aliquot of silica nanoparticles. As a simplification, we used an amount of the functionalizing agent that was equivalent to the TEOS used in the synthesis of the silica particles (i.e., we used a large excess of functionalizing agent). Typically, for 100 mL of silica nanoparticles in ethanolic solution (prepared as described above), we added 1.6 mL of N-(3-trimethoxysilylpropyl) aniline (TSPA). The mixture was stirred for 2 h and then refluxed for another 2 h to promote binding between the particles and the TSPA. The particles were then washed by repeated centrifugations and redispersions in Milli-Q water.

We wished to use aniline-terminated SAM coatings to afford oxidizable aniline moieties as surface templates for the growth of polyaniline overlayers. In these studies, we first concentrated 50 mL of the SAM-coated silica cores (3% w/w in H_2O; 125 nm diameters) and redispersed them in 50 mL of 1.2 N aqueous HCl. The dispersion was then equilibrated for 3 h at 0 ˚C. We then added 64 μL of an aqueous solution of $(NH_4)_2S_2O_8$ at 1 g/L, followed by vigorous stirring at 0 ˚C for 30 min. The amount of initiator added was chosen to correspond to the number of aniline moieties present on the surface of the silica particles (i.e., the concentration was estimated to be 7×10^{12} particles/mL, and the density of moieties was estimated to be 4-5 silanol/nm^2) [24]. The aniline was added at concentrations ranging from 0.001 to 3 g/L. The mixture was stirred overnight to afford a dark green precipitate. The green powder was purified by repeated centrifugations and redispersions in Milli-Q water.

Preparation of CuO-coated silica cores and subsequent polyaniline shell growth

A 20-mL aqueous solution of $Cu(NO_3)_2$ (4.85 g/L) was added to a solution of silica particles (0.1% w/w in 1×10^{-3} N aqueous HCl). The resulting suspension was stirred for 90 min and then aged for 3 h at 120 ˚C. After aging, the particles were centrifuged and washed three times with 1×10^{-3} N aqueous HCl. The resulting pellet was calcined at 800 ˚C for 3 h to fully oxidize the copper. The resultant light green particles were analyzed by SEM.

We hypothesized that oxidant-primed silica cores would promote oxidation on the nanoparticle surface rather than randomly in solution, thereby grafting the conducting polymer onto the surface. In these studies, 100 mg of oxidant-functionalized 250-nm silica cores were dispersed into 50 mL of 1.2 N aqueous HCl, affording a 2% solution by weight. The resulting dispersion was stirred for 30 min in a thick-walled glass vessel. For the CuO oxidant-primed silica particles, 1.5 g of aniline was added, and the vessel was sealed. The mixture was then stirred at 80 ˚C for 48 h. The final light green composite particles were purified by repeated centrifugations and redispersions in Milli–Q water.

Preparation of sterically stabilized silica cores and subsequent polyaniline shell growth

A typical recipe to coat the silica particles with the polymeric stabilizers poly(vinyl alcohol) (PVA), poly(vinyl pyrrolidone) (PVK 30), poly(ethylene glycol) (PEG), and methoxy-capped poly(ethylene glycol) methacrylate (MeOPEGMA) was comprised of the following steps. A mixture of 0.5 mL of ethanol and 3.5 mL of water was added to 10 mg of dry silica particles. The solution was vigorously stirred for 3 h for equilibration. An aliquot (2 mL)

of a solution of the polymeric steric stabilizer (1% w/w in ethanol) was then added, and the mixture was stirred for 4 h at room temperature. Finally, to ensure grafting of the polymer on the silica surface and to increase the number of hydrogen bonds [25], the solution was heated at 80 ˚C for 8 h. The particles were then washed with Milli-Q water to remove any excess stabilizer. The presence of the polymer chains was confirmed by infrared spectroscopy (data not shown).

Polyaniline-coated sterically-stabilized silica-core composites were prepared via the direct oxidation of aniline in the presence of the stabilized silica cores. The use of two distinct oxidizing agents was examined: ammonium persulfate ($(NH_4)_2S_2O_8$) and Fenton's reagent (Fe^{2+}/H_2O_2). Typically, a 1.2 N aqueous HCl solution of silica particles (3% w/w) was stirred at 0 ˚C for 30 min. The oxidant was then added to the solution followed by the addition of aniline. The oxidant/aniline ratio was held constant at 1.25 equivalents, and the concentration ranged from 0.001 to 3 g/L. The reaction was allowed to proceed overnight. Purification of the resultant particles was achieved by repeated centrifugations and redispersions in Milli-Q water.

Preparation of submicrometer polystyrene cores

Polystyrene cores having 750 nm diameters were prepared by emulsion polymerization in an aqueous medium. Typically, 150 mL of Milli-Q water and 200 mg of sodium dodecyl sulfate were combined in a three-necked round-bottomed flask and vigorously stirred. The mixture was then degassed by bubbling with nitrogen for 30 min at 70 ˚C and kept under an atmosphere of nitrogen for the duration of the reaction. A mixture of 20 g of styrene (purified by passage through activated alumina) was added to the heated solution, followed by the addition 0.4 g of potassium persulfate initiator. The emulsion was then stirred for 20 h. Completion of the reaction was confirmed by gravimetry, which involved taking a 1-mL aliquot of the reaction mixture, adding a drop of hydroquinone, heating the mixture, and then measuring the amount of solid [26]. Varying the monomer/initiator ratio and the concentration of monomer in aqueous solution afforded control over the size of the particles, which were purified in dialysis bags (cutoff = 40,000 Daltons), which were bathed for two weeks in periodically replenished Milli-Q water. The particles were then characterized by SEM.

Submicrometer polystyrene cores stabilized with PVK 30

In this method, the steric stabilizer was incorporated during the polymerization reaction. This approach has the advantage of having the polymeric stabilizers firmly anchored onto the surface of the latex; however, since a portion of the stabilizer chain becomes embedded in the latex, the stabilization capacity might be diminished. Typically, 150 mL of Milli-Q water and 200 mg of sodium dodecyl sulfate were stirred vigorously in a three-necked round-bottomed flask. The mixture was degassed by bubbling with nitrogen for 30 min at 70 ˚C. A mixture of 20 g of styrene (purified by passage through activated alumina) and half of the required amount of initiator (0.2 g) was then added. After 4 h of reaction, 30 mL of an aqueous solution of steric stabilizer (20% w/w) was added. After homogenization of the solution, the remaining 0.2 g of the initiator was added. The reaction was then stirred for another 16 h. The particles were purified in dialysis bags as described above, and then characterized by SEM.

This method, based on the process used to prepare sterically stabilized silica particles (*vide supra*), involves grafting of the steric stabilizer onto the surface of the latex after the polymerization has been completed. Typically, 8 g of steric stabilizer was added to 50 mL of a 9% (w/w in H_2O) solution of 800-nm polystyrene particles prepared by emulsion polymerization. The solution was stirred for 3 h at 30 ˚C to enhance the grafting. The resultant particles were purified in dialysis bags as described above, and then characterized by SEM.

Polystyrene cores >1 μm in diameter stabilized with PVK 30

For micron-sized particles, the mechanism of formation of the latex particles differs significantly. The spherical shape of the particle is achieved by the formation of tiny droplets of monomer in the dispersion medium using strong agitation, during

which polymerization takes place. Typically, 120 mL of isopropanol were introduced and combined with 2.1 g of polyvinylpyrrolidone (K30 or K15) in a three-necked round-bottomed flask. The mixture was mechanically stirred until the solid completely dissolved. The solution was then stirred and degassed by bubbling with nitrogen for 30 min at 70 ˚C. A mixture of 15 g of styrene (purified by passage through activated alumina) and 0.15 g of azobisisobutyronitrile (AIBN) was added to the heated mixture under nitrogen. The reaction mixture was stirred vigorously for 24 h to afford a solution with a milky consistency. After cooling, the stabilized latex particles were purified by repeated centrifugation and redispersion with 180 mL of Milli-Q water. The particles were then analyzed by SEM.

Preparation of polyaniline shell / polystyrene core composite nanoparticles

The composite particles were prepared by the oxidative polymerization of aniline in an aqueous solution of the polystyrene cores. Several parameters were systematically varied to establish the optimum conditions for coating the polystyrene particles with polyaniline. Specifically, the oxidants used were H_2O_2/Fe^{3+} and $(NH_4)_2S_2O_8$, the concentration of latex particles was varied from 5 to 20% (w/w in H_2O), the concentration of aniline was varied from 0.05 to 9 g/L, the polystyrene core particles ranged in size from 700 nm to 2.5 μm, and the surfaces of the various polystyrene cores were pretreated separately with ionic and steric stabilizers. Typically, the dry particles or latex solutions were dispersed in 1.2 N aqueous HCl. The solution was then cooled in a round-bottomed flask at 0 ˚C and stirred for 30 min. The oxidant was added, and the mixture was stirred for an additional 30 min at 0 ˚C. Finally, freshly distilled aniline was added to the flask. The oxidant/aniline ratio was held constant at 1.25 equivalents. The reaction was stirred overnight to afford a dark green suspension, which was purified by repeated centrifugations and redispersions in Milli-Q water. The most reproducible uniform coatings were prepared using the following parameters: Typically, 1 g of dry polystyrene particles (1.6 μm diameter) was dissolved in 1.2 N aqueous HCl through sonication. The milky solution was then cooled at 0 ˚C for 30 min. An aliquot (765 mg) of $(NH_4)_2S_2O_8$ was added with vigorous stirring, and 0.25 g of aniline was then introduced to the mixture at 0 ˚C. The solution turned green over the course of 30 min. The solution was stirred overnight under nitrogen. The green solution was then centrifuged to afford a green pellet, which contained the polystyrene cores coated with polyaniline.

Preparation of polypyrrole shell / silica core composite nanoparticles

Freshly distilled pyrrole was chemically polymerized by atmospheric O_2 at 80 ˚C in the presence of 480-nm silica particles (3% w/w in H_2O). Both bare and sterically-stabilized silica particles were investigated. The reaction was allowed to proceed for 64 h in a tightly sealed thick-walled glass vessel. The concentration of pyrrole was varied from 0.001 to 3 g/L. The resultant nanoparticles were purified by repeated centrifugations and redispersions in Milli-Q water.

Freshly distilled pyrrole was polymerized *in situ* with silica particles and iron chloride. The $FeCl_3$ was added to a 3 wt% solution of 480-nm silica particles in 1.2 N aqueous HCl at 0 ˚C. The yellow mixture was stirred for 30 min for equilibration, and then the pyrrole monomer was added to the solution in concentrations ranging from 0.001 to 3 g/L. The oxidant/monomer ratio was held constant at 1.25 equivalents. The resultant dark black particles were purified by repeated centrifugations and redispersions in Milli-Q water.

Preparation of polypyrrole shell / polystyrene core composite nanoparticles

After establishing the optimum conditions for the growth of polyaniline shells on polystyrene cores (*vide supra*), we explored the growth of polypyrrole shells on polystyrene cores using the following typical recipe. A 50 mL aliquot of 1.2 N aqueous HCl was added to 1 g of dry latex particles stabilized with PVK 30. The mixture was dispersed by sonication for 30 min and then cooled at 0 ˚C. An aliquot (750 mg) of anhydrous $FeCl_3$ was added to the solution. After 30 min of equilibrium, 250 mg of pyrrole was added to the flask. The solution was stirred overnight to afford a solution containing black precipitates. The black shells were purified through repeated centrifugations and redispersions in Milli-Q water.

RESULTS AND DISCUSSION

Polyaniline-Coated Particles

After making the silica core particles, we explored several methods of coating them with polyaniline shells such as SAM-functionalized, oxidant-primed, sterically stabilized and bare silica cores. Unfortunately, the polymerization of aniline in the presence of SAM-coated, oxidant-primed, sterically-stabilized and submicrometer silica cores failed to yield the desired shell/core particles. Analysis by SEM (Figure 1a,b,c,d) showed that, instead of forming discrete polymer-coated silica particles, these strategies afforded silica cores embedded in

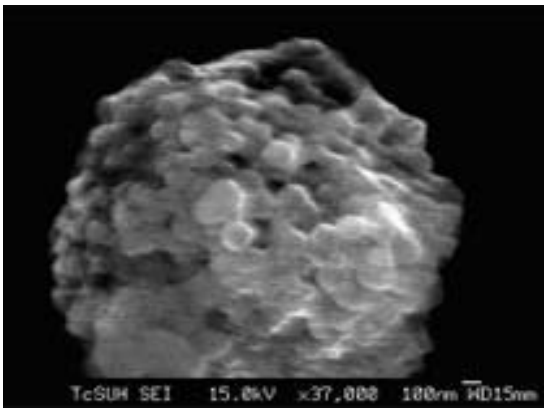

(a)

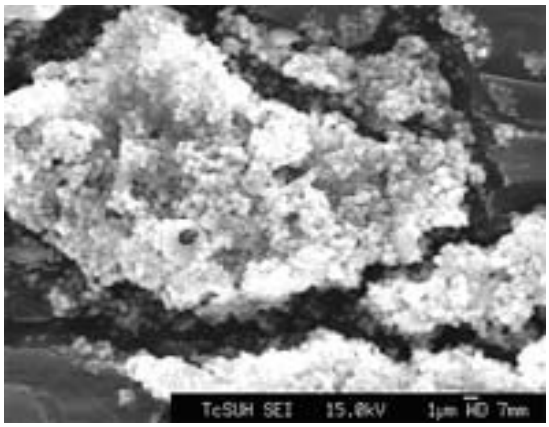

(b)

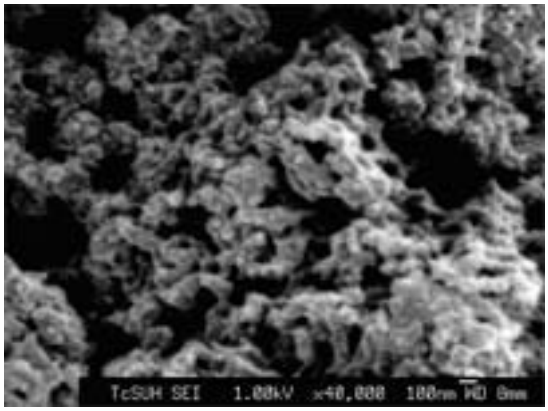

(c)

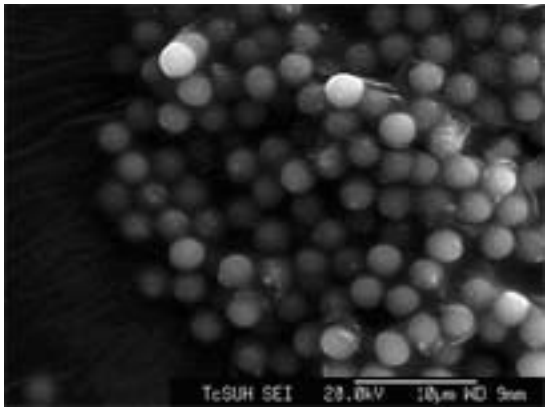

(d)

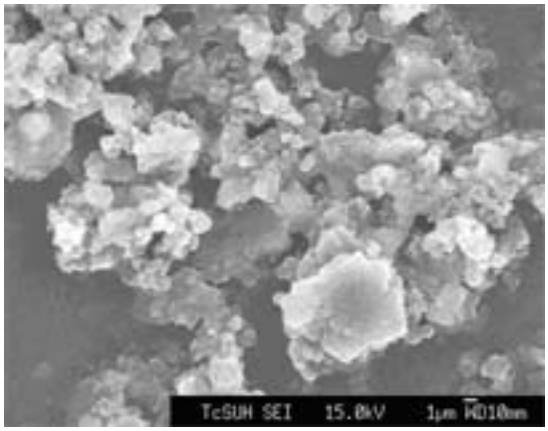

(e)

Figure 1. SEM images of polyaniline-coated silica particles: polyaniline growth in the presence of (a) SAM-coated silica cores (b) polyaniline growth in the presence of copper-oxide-primed silica cores (c) polyaniline growth in the presence of sub-micrometer bare silica cores (250 nm in diameter) (d) polyaniline grown in the presence of micrometer bare silica cores (1 μm in diameter) (e) polymerization of aniline in the presence of sterically-stabilized silica cores (620 nm in diameter).

a matrix of polyaniline. However, we note that for the larger bare cores, this method does appear to produce discrete shells around the silica beads, although some degree of aggregation is apparent or only partially embedded in a polyaniline matrix (Figure 1e). As noted above, the outcome of the polymerization of aniline in the presence of silica particles appears to be influenced by the size of the silica cores. With silica cores smaller than one micron, neither steric stabilization nor templated initiation allows for the formation of discrete shell/core geometries.

In addition to the silica cores, we wished to investigate the use of more versatile core particles, such as those composed of latex-polymers. The *in-situ* polymerization of aniline with bare submicrometer polystyrene particles afforded embedded polystyrene particles (Figure 2a). In contrast, polystyrene particles having diameters greater than one micron produced discrete shells, although the quality of the coatings was poor (Figure 2b). However, steric stabilization can be used to prevent coalescence. Indeed, various modes of stabilization for latex suspensions (e.g., adsorbed steric stabilizers and grafted ionic surfactants) have been developed [27]. We wished to investigate the benefit of mixing adsorbed PVK 30 with latex-polymer particles during the attempted growth of conducting-polymer shells. A series of experiments was performed using polystyrene cores ranging in size from 300 nm to 3 μm in diameter. The *in-situ* polymerization of aniline with ~800 nm polystyrene particles (Figure 2c) stabilized with PVK 30 offered a matrix of polystyrene cores embedded in polyaniline (Figure 2d). Compared to analogous experiments using non-sterically-stabilized cores (Figure 2a), the sterically- stabilized cores formed smaller aggregates, showing the efficacy of the stabilizing agent. Despite several attempts using various steric stabilizers and reaction conditions, we were unable to produce discrete polyaniline-coated particles when using sub-micrometer latex cores. In contrast, the use of micometer-sized latex cores (Figure 2e) in concert with steric stabilizers (PVK 30) afforded discrete polyaniline-coated composite particles (Figure 2f).

Polypyrrole-coated particles

The oxidative polymerization of pyrrole requires milder oxidizing conditions than does aniline [28]. As a starting point, we based our initial studies on work by Matijevic *et. al.* [15], who established a methodology for preparing polypyrrole-coated silica particles. By analogy, we explored the use of two separate oxidizing agents for initiating the polymerization: $FeCl_3$ and atmospheric O_2.

The polymerization of pyrrole with the two initiators in the presence of the silica cores led to the formation of a black precipitate, which consisted of silica particles embedded in a matrix of polypyrrole (Figure 3a,b). The electron micrograph for the oxygen run (Figure 3b) shows a few discrete shell/coreparticles. It is possible that the use of $FeCl_3$ leads to the incorporation of high valency Fe^{3+} ions, which can destabilize the shell/core structure [29]. As described in the preceding section, the polymerization of pyrrole *in-situ* with bare silica particles afforded a few discrete shells when using O_2 as the initiator. We thus sought to enhance the coating process by adding a stabilizing agent to prevent aggregation of the silica particles. Indeed, the use of polyvinyl-alcohol as a steric stabilizer led to colloidal stability (Figure 3c). Polypyrrole shells were grown on submicron and micron-sized particles. These results contrast with those of the polyaniline studies, where the silica particles remained entrenched in a polyaniline matrix despite the use of steric stabilizers.

Given the success of the previous syntheses using steric stabilizers, we chose to forego attempts to coat bare sub-micrometer polystyrene cores with polypyrrole. Instead, our initial efforts relied on the method of Lascelles *et al.* forgrowing polypyrrole films on sterically-stabilized micron-sized latex particles [30]. This method affords a collection of particles that appear as a powder with an intense black color. The electron micrographs illustrate the presence of a shell/core geometry with a thin layer of polypyrrole as the shell (Figure 3d, e).

Optical properties of the polyaniline- and polypyrrole-coated cores

The attractive materials properties of conducting polymers, such as (1) optical absorptions in the visible and near-infrared spectral regions, (2) enhanced conductivities in either oxidized or reduced states, and (3) reversible redox behavior, are derived from the extended π conjugation along the polymer backbones [31]. Incident radiation

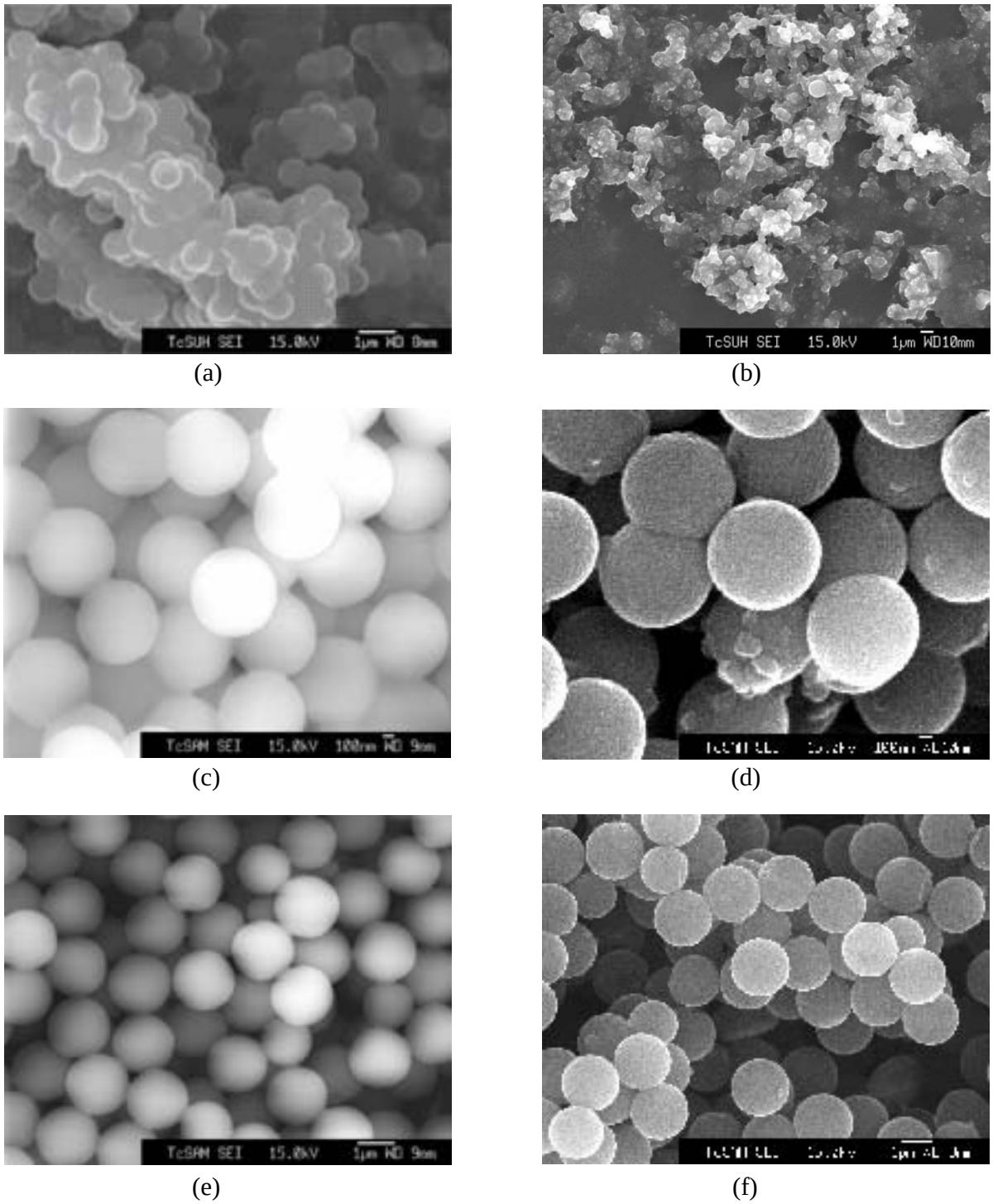

(a) (b)

(c) (d)

(e) (f)

Figure 2. SEM images of polyaniline-coated polystyrene particles: (a) sub-micrometer bare polystyrene particles (b) polystyrene/divinyl-benzene particles coated with polyaniline (c) sub-micrometer polystyrene cores (~800 nm) stabilized with PVK 30 (d) polyaniline coated with sub-micrometer polystyrene cores (~800 nm in diameter) stabilized with PVK 30 (e) micrometer polystyrene particles (1.6 μm in diameter) stabilized with PVK 30 (f) polyaniline-coated PVK 30-stabilized micrometer polystyrene cores (1.6 μm in diameter).

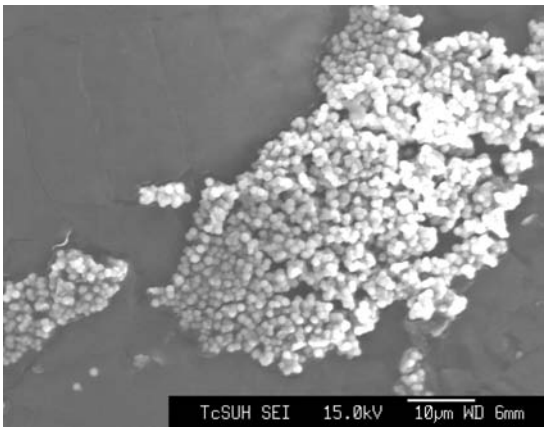

(a)

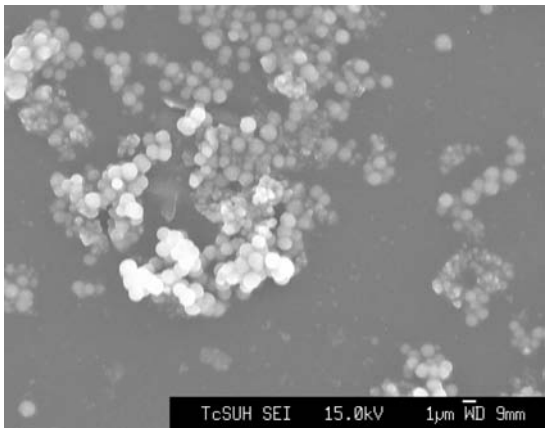

(b)

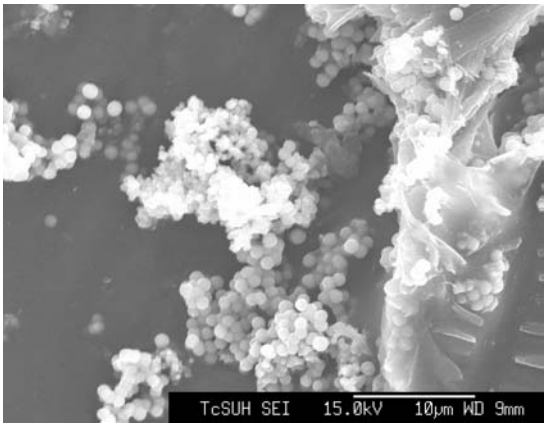

(c)

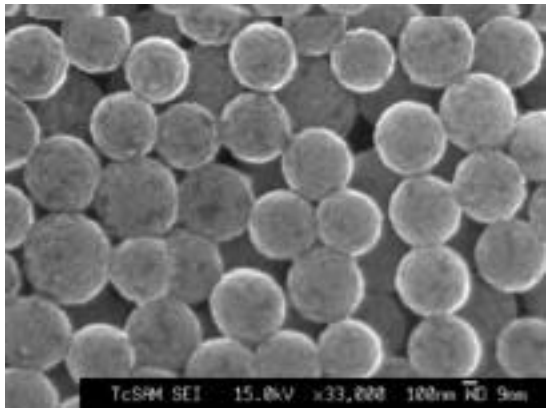

(d)

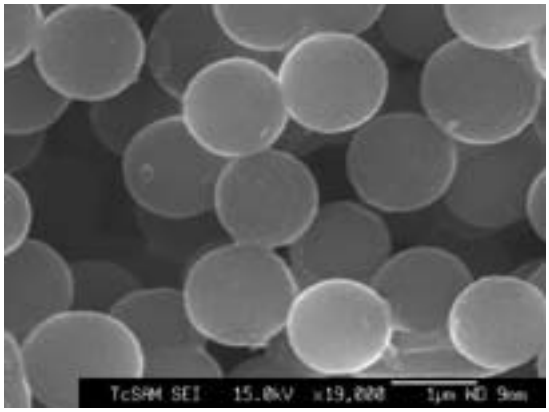

(e)

Figure 3. SEM images of polypyrrole-coated silica and polystyrene particles: (a) polypyrrole growth in the presence of bare silica cores (480 nm in diameter) using $FeCl_3$ as the initiator (b) polypyrrole grown in the presence of bare silica cores (480 nm in diameter) using O_2 as the initiator (c) PVA-stabilized silica cores (480 nm in diameter) coated with polypyrrole (d) PVK 30-stabilized sub-micrometer polystyrene cores (~800 nm in diameter) coated with polypyrrole (e) PVK 30-stabilized micrometer polystyrene cores (1.6 μm in diameter) coated with polypyrrole.

interacts not only with electronic and bond-vibrational excitations, but also with free carriers in the polymer conduction band. Collectively, these interactions give rise to phenomena such as free-carrier absorption, Fermi-level excitation, and light-scattering by free electrons [32].

As described in the introduction, we are exploring the preparation and study of conducting polymer-coated dielectric particles because of their potential to exhibit tunable plasmon resonances in the near infrared spectral region [33]. Mathematical algorithms developed by Halas and co-workers can be used to predict the precise band position of these plasmon resonances as a function of the shell thickness and dielectric core size [34].

Given these motivations, we performed a thorough experimental characterization of the optical properties of composite conducting-polymer shell / dielectric-core particles, with a particular emphasis on studying the position and magnitude of their plasmon band. Conducting polymers exhibit various absorption bands ranging from 175 nm to 3000 nm (or 0.41 eV to 7.0 eV) [35]. According to literature reports, the plasmon resonance for intrinsically conducting polymer thin films appears in the 620 to 2480 nm (or 0.5 eV to 2 eV) spectral region. We wished to explore whether the conducting-polymer shell / dielectric core geometry is an effective architecture for tuning the plasmon resonance in the near infrared spectral region. We thus compared the UV-vis and near-to-mid infrared signatures of the composite particles to those of their fully characterized bulk counterparts [36-38].

We collected the IR spectra of bulk polyaniline, bare silica particles, and polyaniline-coated silica cores (Figure 4). The characteristic vibrational bands of polyaniline are: υ(C=C) 1600 cm^{-1}, υ(C=C) quinone deformation (1580 cm^{-1}), υ(C=C) benzene deformation (1490 cm^{-1}), υ(C-N) stretching (1310 cm^{-1}), υ(-NH^{+}=) vibration (1140 cm^{-1}), and υ(C-H) out-of-plane bending (812 cm^{-1}) [39,40]. Similarly, those of silica are: υ(O-H) stretching (3500 cm^{-1}), υ(O-H) bending (1600 cm^{-1}), υ(Si-O-Si) rocking (1110 cm^{-1}), υ(Si-O) asymmetric Si-O stretching (1100 cm^{-1}), and υ(Si-O) symmetric stretching (800 cm^{-1}) [41,42]. Figure 4 shows that the strong IR bands of the silica core completely dominate the spectrum of the composite particle, even though analysis by SEM (*vide supra*) and UV-vis (*vide infra*) provides conclusive support for the presence of the polyaniline overlayer.

We also collected the IR spectra of bulk polyaniline, bare polystyrene particles, and polyaniline-coated polystyrene cores (Figure 5). The characteristic IR bands of polystyrene are:

υ(C-H) alkane stretch (3030-3060 cm^{-1}), υ(C-H) alkene stretch (2930 cm^{-1}), υ(C-C) stretch, and

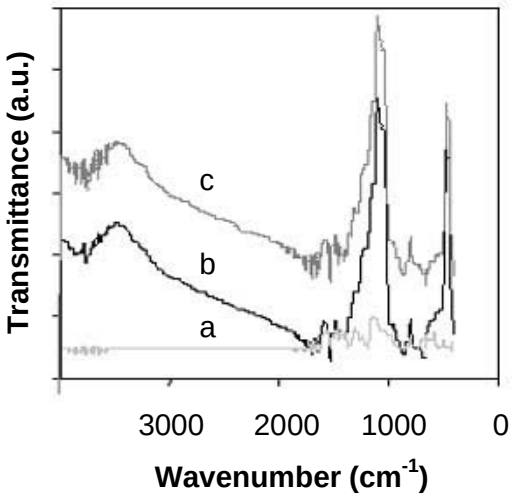

Figure 4. Infrared spectra of (a) bulk polyaniline, (b) polyaniline-coated silica cores (250 nm) prepared using 0.001 g/L of aniline, and (c) bare silica cores (250 nm).

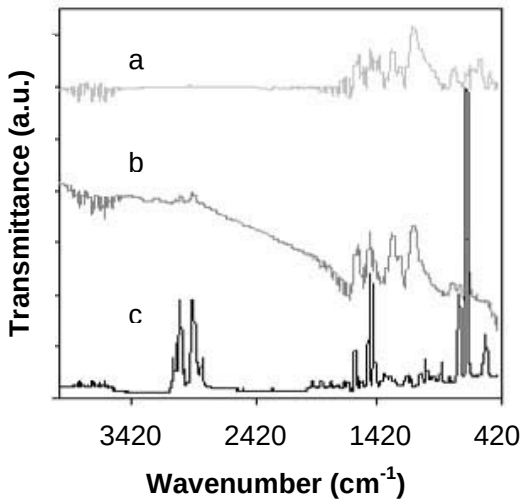

Figure 5. Infrared spectra of (a) bulk polyaniline and (b) polyaniline-coated polystyrene cores (1.6 μm) prepared using 3 g/L of aniline, and (c) bare polystyrene cores (1.6 μm).

benzene fingerprints (1490-1600 cm^{-1}) [43]. Figure 5 shows the partial screening of the vibrational bands of the polystyrene cores by the polyaniline coating. Thus, in addition to UV-vis spectroscopy (*vide infra*), IR spectroscopy offers supporting evidence for the formation of polyaniline-coated polystyrene cores.

Separately, we collected the IR spectra of bulk polypyrrole, bare silica particles, and polypyrrole-coated silica cores (Figure 6). The characteristic vibrational bands of polypyrrole are: υ(C-H) stretch (3110 cm^{-1}), υ(C=C) stretch (1540–1410 cm^{-1}), υ(C-N) stretch (1480 cm^{-1}), υ(C-C) in–ring stretch and υ(C=C) stretch and υ(C=C-C) ring-in-plane deformation (1350-1330 cm^{-1}), υ(C-H) ring-out-of-plane bending and υ(C-C) inter-ring-out-of-plane bending and υ(N-H) and υ(C=C)-N ring-out-of-plane deformation (1050-1040 cm^{-1}). Figure 6 shows that the strong IR bands of the silica core (detailed above) completely dominate the spectrum of the composite particle, despite the fact that analyses by SEM (*vide supra*) and UV-vis (*vide infra*) support the presence of the polypyrrole coating.

We also collected the IR spectra of bulk polypyrrole, bare polystyrene particles, and polypyrrole-coated polystyrene cores (Figure 7). As previously noted with polyaniline-coated polystyrene particles, the polystyrene vibrational bands are partially screened by the vibrations from the polypyrrole coating. Thus, in addition to the

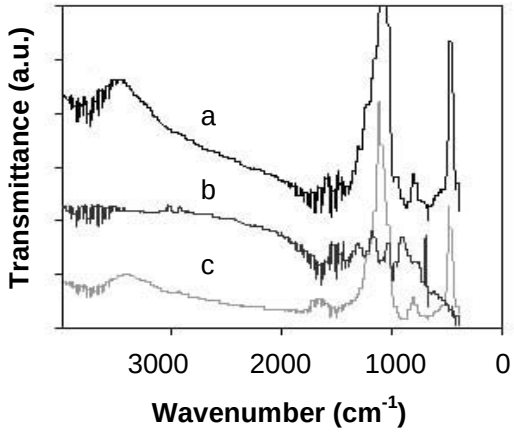

Figure 6. Infrared spectra of (a) polypyrrole-coated silica cores (480 nm) prepared using 0.001 g/L of pyrrole, (b) bulk polypyrrole, and (c) bare silica particles (480 nm).

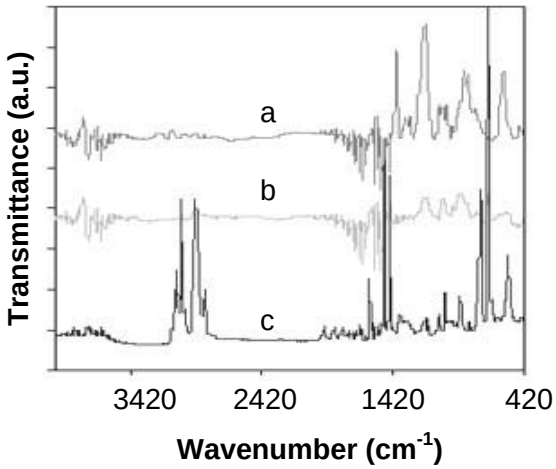

Figure 7. Infrared spectra of (a) bulk polypyrrole, (b) polypyrrole-coated polystyrene cores (1.6 μm) prepared using 3 g/L of aniline, and (c) bare polystyrene particles (1.6 μm).

UV-vis spectra (*vide infra*), the IR spectra indicate the presence of a thin coating of polypyrrole on the polystyrene cores.

The observation that increasing the amounts of monomer and oxidant in the shell-growth reaction led to a decrease in the intensity of the IR bands of the core particles might be interpreted to indicate an increase in shell thickness; however, we observed a similar phenomenon for blends of polyaniline or polypyrrole powders with both types of core particles (Figure 8). Thus, the progressive disappearance of the IR bands of the core particles fails to provide irrefutable evidence of the quality or the extent of the polymer coverage. Furthermore, the infrared spectra of the conducting-polymer / dielectric core particles are indistinct from those of bulk conducting polymer samples. In light of these results, we conclude that the extent and quality of polymer coverage cannot be assessed by infrared spectroscopy.

As noted above, the exposure of conjugated polymers to UV-vis light triggers numerous optical absorptions arising from the multitude of electronic configurations (e.g., polarons and bipolarons, with varying degrees of doping) along the backbone. To characterize the optical properties of the composite particles, we collected their UV-vis spectra both in solution and in the solid state using ATR. The solution spectra are shown in Figure 9. For undoped polyaniline (i.e., the emeraldine base), the characteristic absorption

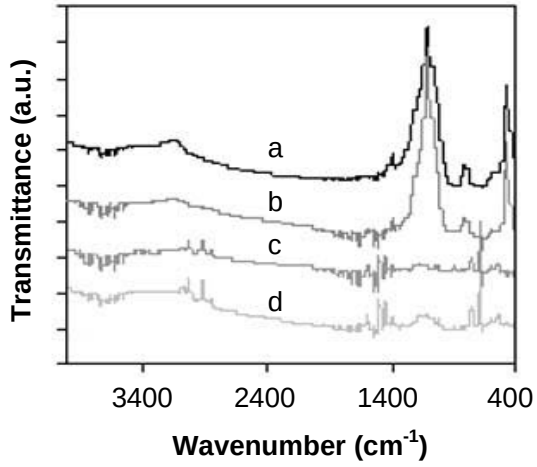

Figure 8. Infrared spectra of blends of the mixture of (a) silica particles and polyaniline, (b) silica particles and polypyrrole, (c) polystyrene particles and polyaniline, and (d) polystyrene particles and polypyrrole. These blends used polymer/core ratios comparable to those of the composite particles.

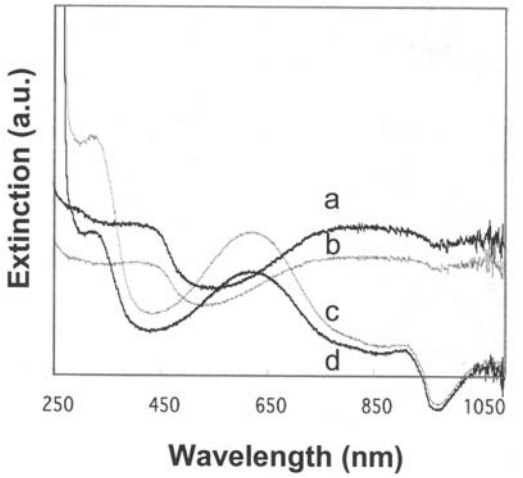

Figure 9. Extinction spectra of (a) doped bulk polyaniline, (b) doped polyanilline-coated silica cores (1 μm), (c) undoped bulk polyaniline, and (d) undoped polyaniline-coated silica cores (2.5 μm). Spectra of undoped samples were collected in DMF and those of doped samples were collected in H_2SO_4, which served as the dopant.

bands are the π–π* transition of the conjugated backbone at 333 nm (3.5 eV) and the exciton centered on the quinoid ring at 620 nm (2 eV) [44]. Both bands are readily apparent in the spectra of bulk polyaniline (c) and the polyaniline-coated silica cores (d).

Upon protonation, excitation of the valence electrons to the half-filled lower polaron generates a new absorption band at ~490 nm (~2.50 eV) [44, 45]. Through electronic reorganization, the quinoid feature is no longer present for either doped bulk polyaniline (a) or the doped polyaniline-coated silica cores (b). The spectra also exhibit a broad absorption starting at ~670 nm (~1.85 eV) and extending to longer wavelengths that can be assigned to multiple excitations principally composed of polaron excitations and a free-carrier plasmon resonance [38]. For the latter band, the features we observed are consistent with those reported previously for bulk polyaniline doped with H_2SO_4 [37, 38]. While one might argue that, for the shell/core structures, the band at ~490 nm is slightly red-shifted and the longer wavelength band is slightly blue-shifted, we can draw no concrete conclusions from these data given the small magnitude of the differences and the likelihood of differences in sample concentration and/or doping levels.

The corresponding UV-vis ATR spectra of the doped materials also exhibit absorption bands at ~490 nm and at ~670 nm with extension to longer wavelengths (Figure 10). Again for the shell/cores structures, the band at ~490 nm is slightly red-shifted and the longer wavelength band is slightly blue-shifted relative to that of bulk polyaniline. As noted above, we can draw no firm conclusions from these small differences [37, 38].

For the polystyrene cores, we also collected solution and solid-state UV-vis spectra (Figures 11 and 12). For both sets of spectra, the characteristic absorption bands of the polyaniline-coated polystyrene cores are similar to those described above for the bulk polyaniline, except for small shifts in wavelength comparable and analogous to those reported above for the polyaniline-coated silica cores. Given these data as a whole, we have been unable to demonstrate that the shell/core architecture, when comprised of polyaniline shells and either silica or polystyrene cores, can be used to tune the position of the broad absorption band at ≥ 670 nm, which has been attributed to multimode excitations (including the plasmon resonance) of polyaniline [38]. We note, however, that other optical features derived from a Kramers-Kronig analysis of the reflective data have yet to be examined [46].

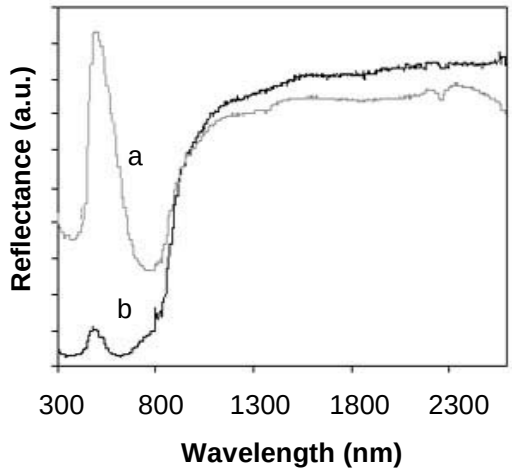

Figure 10. Attenuated total reflectance UV-vis spectra of (a) doped bulk polyaniline and (b) doped polyaniline-coated silica cores (2.5 μm). The latter samples were prepared using 3 g/L of aniline; both samples were doped with H_2SO_4.

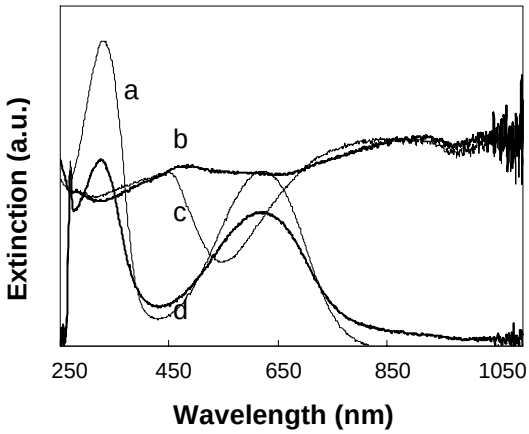

Figure 11. Extinction spectra of (a) undoped bulk polyaniline, (b) doped bulk polyaniline (c) undoped polyaniline-coated polystyrene cores (1.6 μm), and (d) doped polyaniline-coated micrometer polystyrene cores (1.6 μm). Spectra of undoped samples were collected in DMF and those of doped samples in H_2SO_4, which served as the dopant.

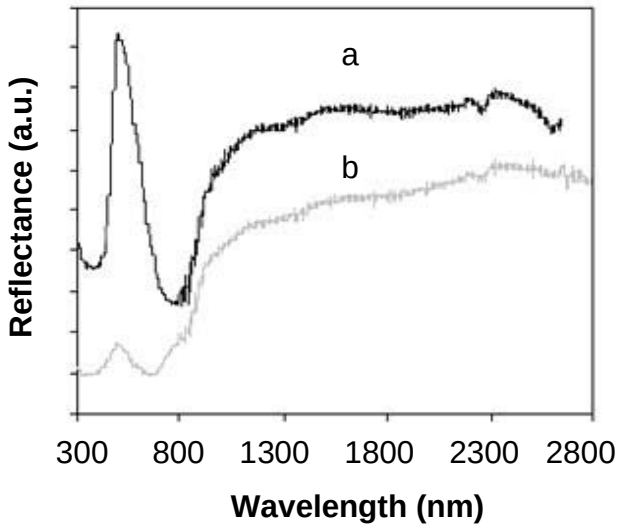

Figure 12. Attenuated total reflectance UV-vis spectra of (a) doped bulk polyaniline and (b) doped polyaniline-coated micrometer polystyrene cores (1.6 μm). The latter samples were prepared using 5 g/L of aniline; both samples were doped with H_2SO_4.

Given the poor solubility of polypyrrole and polypyrrole-coated core particles, we were unable to collect their UV-vis spectra in solution. We were, however, able to collect solid-state ATR UV-vis spectra of bulk polypyrrole and of the polypyrrole-coated core particles. All of the samples, which are inherently doped [9], exhibit a broad absorption band starting at ~730 nm (~1.7 eV) and extending to longer wavelengths (Figures 13 and 14). The position and appearance of this band,

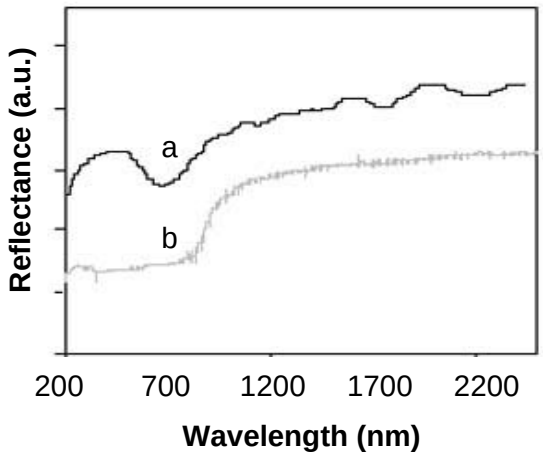

Figure 13. Attenuated total reflectance UV-vis spectra of (a) bulk polypyrrole and (b) polypyrrole-coated silica cores (480 nm). The latter were prepared using 4 g/L of pyrrole.

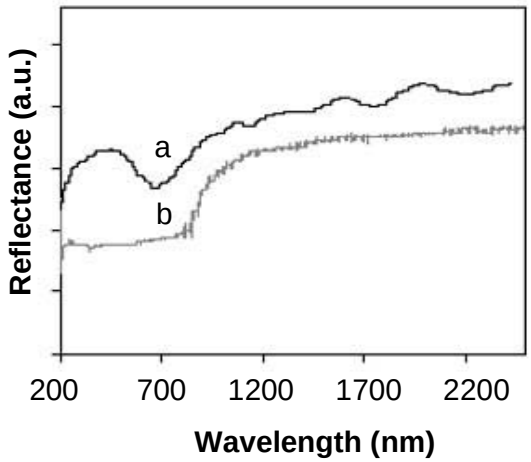

Figure 14. Attenuated total reflectance UV-vis spectra of (a) bulk polypyrrole and (b) polypyrrole-coated polystyrene cores (1.6 μm). The latter were prepared using 4 g/L of pyrrole.

which arises from multimode excitations (including the plasmon resonance) [47], is in agreement with previous studies [37].

As observed with the polyaniline system, there are small shifts in the position of the absorption bands when comparing the polypyrrole-coated cores to bulk polypyrrole. The shifts here for the composite particles are toward longer wavelengths (i.e., red-shifted) when compared to the bulk conducting polymer. We note, however, that the magnitude of the shifts is quite small and might be due to experimental artifact (e.g., differences in sample preparation). Consequently, we are unable to draw any firm conclusions regarding whether the shell/core architecture can be used to tune the position of the absorption bands. A detailed Kramers-Kronig analysis of the reflective data might provide a better understanding of the optical properties of these unique systems [46].

CONCLUSIONS

We have established reliable conditions for preparing composite nanoparticles in which a dielectric core is coated with a thin conducting polymer shell. The ability to prepare the particles was found to be independent of the composition of the cores (i.e., both silica and polystyrene cores were successfully used), but strongly dependent on the size of the core and the nature of the conducting polymer. For example, attempts to grow polyaniline on submicrometer cores typically led to aggregation and precipitation of the composite particles. Specifically, silica cores with diameters varying from 125 to 680 nm consistently failed to produce discrete polymer-coated particles, even when using SAM-coated silica cores, oxidant-primed silica cores, and sterically-stabilized silica and polystyrene cores. The difficulty associated with the use of submicron cores is likely due to the initial oligomers formed in the polymerization of polyaniline, which crosslink the smaller particles. On larger particles, the oligomers might be adsorbed entirely on the surface of the particles, thus preventing the aggregation phenomenon. In contrast to the results with polyaniline, we found it possible to grow polypyrrole coatings on submicron silica cores. Specifically, we were able to grow discrete polypyrrole-coated silica cores having diameters ranging from 250 to 680 nm. When using cores above the micron threshold, however, we found that it was possible to grow thin polyaniline and polypyrrole coatings on both silica and polystyrene cores. In particular, the use of steric stabilizers led to composite particles with smooth surfaces. The most reliable results for both polyaniline and polypyrrole coatings were achieved using 1.6 μm polystyrene cores grafted with PVP as the steric stabilizer. Infrared spectroscopic analysis of the composite particles supported the formation of the shell/core structure,

but failed to provide a reliable measure of the thickness of the conducting particle overlayer. Analysis by UV-vis spectroscopy revealed that the adoption of the shell/core architecture exerts little or no influence upon the optical properties of doped polyaniline and polypyrrole in the UV-vis to near-infrared region.

ACKNOWLEDGMENT

We gratefully acknowledge financial support from the Army Research Office, the Texas Center for Superconductivity, and the Robert A. Welch Foundation (Grant E-1320).

REFERENCES

1. Grice, W. P., U'Ren, A. B., and Walmsley, I. A. 2001, Phys. Rev. A, 64, 6381.
2. Kaminow, I. P. 1974, An Introduction to Electro-optic Devices, Academic: New York.
3. Hermann, J. P., and Ducing, J. 1974, J. Opt. Commun., 10, 258.
4. Partch, R. E. 1997, In Material Synthesis and Characterization, Perry, D. (Ed.), Plenum: New York.
5. Hofman-Caris, C. H. M. 1994, New J. Chem., 18, 1087.
6. Liz-Marzan, L. M., Giersig, M., and Mulvaney, P. 1996, Langmuir, 12, 4329.
7. Matijevic, E. 1996, In Fine Particle and Science Technology, Pelizetti, E. (Ed.), Kluwer: Dordrecht, The Netherlands.
8. Davies, R., Schurr, G. A., Meenan, P., Nelson, R. D., Bergna, H. E., Brevett, C. A. S., and Goldbaum, R. H. 1998, Adv. Mater., 10, 1264.
9. Nalwa, H. S. 1997, Handbook of organic conductive molecules and polymers, Volume 3 conductive polymers: spectroscopy and physical properties, Wiley, New York.
10. Delpy, D. T., and Cope, M. 1997, Phil. Trans. Roy. Soc. Lond. B. Bio. Ser., 352, 649.
11. Oldenburg, S. J., Hale, G. D., Jackson, J. B., and Halas, N. J. 1999, Appl. Phys. Lett., 75, 1063.
12. Jackson, J. B., and Halas, N. J. 2001, J. Phys. Chem. B, 105, 2743.
13. Tom, R. T., Nair, A. S., Singh, N., Aslam, M., Nagendra, C. L., Philip, R., Vijayamohanan, K., and Pradeep, T. 2003, Langmuir, 19, 3439.
14. Wang, H., Brandl, D. W., Le, F., Nordlander, P., and Halas, N. J. Nano Lett., ACS ASAP.
15. Jiang, Z. J., and Liu, C. Y. 2003, J. Phys. Chem. B., 107, 12411.
16. Shi, W., Sahoo, Y., Swihart, M. T., and Prasad, P. N. 2005, Langmuir, 21, 1610.
17. Bremer, L. G. B., Verbong, M. W. C. G., Webers, M. A. M., and Doorn, M. A. M. M. 1997, Synth. Met., 84, 355.
18. Cairnes, D. B., Armes, S. P., and Bremer, L. G. B. 1999, Langmuir, 15, 8052.
19. Huang, C. L., and Matijevic, E. 1995, E. J. Mater. Res., 10, 1327.
20. Rusa, M., Whitesell, J. K., and Fox, M. A. 2004, Macromolecules, 37, 2766.
21. Barthet, C., Armes, S. P., Chehimi, M. M., Bilem, C., and Omastova, M. 1998, Langmuir, 14, 5032.
22. Stöber, W., and Fink, A. J. 1968, J. Coll. Interf. Sci., 26, 62.
23. Van Helden, A. K., Jansen, J. W., and Vrij, A. 1980, J. Colloid and Interface Sci., 81, 354.
24. Wadell, T. G., Leyden, D. E., and DeBello, M. T. 1981, J. Am. Chem. Soc., 103, 5303.
25. Chen, C. W., Chen, M. Q., Serizawa, T., and Akashi, M. 1998, Chem. Comm., 831.
26. Gabaston, L. I., Jackson, R. A., and Armes, S. P. 1998, Macromolecules, 31, 2883.
27. Wu, X., and van de Ven, T. G. M. 1996, Langmuir, 12, 3859.
28. Asavapiriyanont, S., Chandler, G. K., Gunawardena, G. A., and Pletcher, D. 1984, J. Electroanal. Chem., 177, 229.
29. Biggs, S., and Proud, A. D. 1997, Langmuir, 13, 7202.
30. Lascelles, S. F., and Armes, S. P. 1995, Adv. Mater., 7, 864.
31. Bernier, P., Lefrant, S., and Bidan, G. 1999, Advances in Synthetic Metals – Twenty Years of Progress in Science and Technology, Elsevier.
32. Schrader, B. 1995, Infrared and Raman Spectroscopy – Methods and Applications, VCH.
33. Oldenburg, S. J., Averitt, R. D., Westcott, S. L., and Halas, N. J. 1998, Chem. Phys. Lett., 288, 243.
34. Sarkar, D., and Halas, N. J. 1997, Phys. Rev. E, 56, 1102.

35. Rodriguez, J., Grande, H. J., and Otero, T. F. 1997, Handbook of Organic Conductive Molecules and Polymers, Volume 2, John Wiley, Chichester.
36. Ehrenreich, H., and Philipp, H. R. 1962, Phys. Rev., 128, 1622.
37. Lee, K., Heeger, A. J., and Cao, Y. 1995, Synth. Met., 72, 25.
38. Lee, K., Heeger, A. J., and Cao, Y. 1993, Phys. Rev. B, 48, 14884.
39. Stejskal, J., Sapurina, I., Trchová, M., Prokeš, J., IvkaIø, K., and Tobolková, E. 1998, Macromolecules, 31, 2218.
40. Yasuda, A., and Shimidzu, T. 1993, Polym. J., 25, 329.
41. Bjorklund, R. B., and Liedberg, B. 1986, J. Chem. Soc. Chem. Commun., 1986, 1293.
42. Street, G. B., Clarke, T. C., Krounbi, M., Hanazawa, K., Lee, V., Pfluger, P., Scott, J. C., and Weiser, G. 1982, Mol. Cryst. Liq. Cryst., 83, 253.
43. Silverstein, R. M., Bassler, G. C., Morrill, T. C. 1981, Spectrometric Identification of Organic Compounds, 4th ed., Wiley, New York.
44. Cao, Y., Smith, P., and Heeger, A. J. 1989, Synth. Met., 32, 263.
45. Wudl, F., Angus, R. O., Lu, F. L., Allemand, D. M., Vaxhon, D. J., Nowak, M., Liu, Z. X., and Heeger, A. J. 1987, J. Am. Chem. Soc., 109, 3677.
46. Tzamalis, G., Zaidi, N. A., Homes, C. C., and Monkman, A. P. 2001, J. Phys. Condens. Matter, 13, 6297.
47. Kohlman, R. S., Joo, J., Wang, Y. Z., Pouget, J. P., Kaneko, H., Ishiguro, T., and Epstein, A. J. 1995, Phys. Rev. Lett., 74, 773.